Desalination and Water Treatment
www.deswater.com

51 (2013) 830–836
January

doi: 10.1080/19443994.2012.699349

Taylor & Francis
Taylor & Francis Group

Heat transfer performance and bundle-depth effect in horizontal-tube falling film evaporators

Shengqiang Shen*, Gangtao Liang, Yali Guo, Rui Liu, Xingsen Mu

Key Laboratory for Sea Water Desalination of Liaoning Province, Dalian University of Technology, Dalian 116024, China
Tel. +86 0411 84708464; Fax: +86 0411 84707963; email: zzbshen@dlut.edu.cn

Received 1 March 2012; Accepted 10 May 2012

ABSTRACT

A set of experimental facilities were set up to measure overall heat transfer coefficient of horizontal-tube falling film evaporator with square-pitch bundle. Effect of spray density, saturation temperature, total temperature difference, and inlet steam velocity on the overall heat transfer coefficient K is studied. The tubes are made of HAL77-2A aluminum brass with an outer diameter of 25.4 mm. Fluids inside and outside the tubes are steam and fresh water respectively. The results indicate that growth of spray density and saturation temperature helps to increase the K. The K could also be increased by reducing the total temperature difference. However, the impact of the inlet steam velocity on the K is less significant. Furthermore tube bundle-depth effect and space distribution of local overall heat transfer coefficient $\tilde{K}$ in the evaporator are also presented. Based on this investigation, basic engineering design information will be provided to establish the governing parameters for horizontal-tube falling film evaporator in the field of seawater desalination.

Keywords: Horizontal-tube falling film evaporator; Heat transfer coefficient; Bundle-depth effect; Space distribution; Seawater desalination

1. Introduction

Water is a basic substance of life, and it is increasingly in short supply all over the world. It is estimated that water shortage affects 88 developing countries that are home to half of the world's population. In these places, 80–90% of all diseases and 30% of all deaths result from poor water quality [1]. Less than 1% of the world's water sources are considered potable, however, about 97% of water in the world is salty as its chief sources are sea and brackish water [2]. So seawater desalination is known to be an essential available solution for the shortage of fresh water. A seawater desalination process separates saline seawater into two streams: a fresh water stream containing a low concentration of dissolved salts and a concentrated brine stream. This process requires some form of energy to desalinate, and utilizes several different technologies for separation [3]. A variety of desalination technologies have been developed over the years such as multi-stage flash, reverse osmosis, and low-temperature multi-effect distillation (LT-MED). At present, LT-MED has become one of the main commercial seawater desalination technologies due to the advantages such as low corrosion rates,

*Corresponding author.

Presented at the International Conference on Desalination for the Environment, Clean Water and Energy, European Desalination Society, 23–26 April 2012, Barcelona, Spain

flexibility, high thermodynamic efficiency, minimal scaling rates, high-purity distillate, reliability, and low energy costs [4].

Nowadays, falling film evaporation on horizontal tubes is the preferred technique in LT-MED. But the published information that is relevant to the topic is focused on evaporation outside the single tube or the tube bundle. Chyu and Bergles [5] presented experimental data and analytical results for laminar films on a horizontal tube. Parken et al. [6] observed an increase in nonboiling evaporation coefficient with increasing feed water temperature and flow rate. Shen [7] investigated the overall heat transfer coefficient of horizontal-tube falling film evaporator, and results indicated that the heat transfer coefficient increased with the increment of spray density and saturation temperature. Results of Jelino [8] showed that heat flux, spray density and salinity almost had no influences on h_o. Zeng et al. [9] observed an increase in h_o with increasing heat flux and saturation temperature but almost independent of spray density. Zeng et al. [9] suggested that a square-pitch bundle tended to provide a higher heat transfer performance than a triangular-pitch bundle at a low saturation temperature, while at a high saturation temperature, the performance of a triangular-pitch bundle was more likely to be higher. Zeng et al. [10] also indicated the tube bundle effect was insignificant at lower saturation temperature and lower spray density. Fujita and Tsutsui [11] pointed out that with an increase in film flow rate, the heat transfer coefficient at first decreased, then remained nearly constant, and finally increased. The topmost tube had lower heat transfer coefficient compared to the tubes located below it. Liu et al. [12] found that tube positions within the bundle did not have a significant impact on the heat transfer coefficient. According to Lorenz and Yung [13], the single tube results could not properly reflect large bundle because of film breakdown when Re was below 300, but for Re > 300, no bundle-depth variations in the heat-transfer coefficient were observed. However, in the open literature, only a few studies concerning the overall heat transfer coefficient in the falling film evaporators can be found.

This paper discusses the effect of main factors of falling film evaporation and condensation process on the overall heat transfer coefficient, based on the measured data outside and inside the single tube obtained from the experimental facilities separately. Besides, impact of these factors on tube bundle-depth effect and space distribution of heat transfer coefficient in the evaporator is also considered. Details on the three aspects are described in later sections.

2. Experimental apparatus and approaches

To obtain the overall heat transfer coefficient and analyze heat transfer characteristics of inside and outside the tube respectively, two experimental platforms were set up. Fig. 1 shows a simplified schematic diagram of experimental apparatus for the falling film evaporation outside a horizontal tube. This apparatus mainly measures heat transfer coefficient of evaporation outside a single tube. It consists of a heating tank, a constant pressure liquid feeder, testing cell (evaporator), a metering pot, and two condensers. Water is heated to a certain temperature by the main heater in the heating tank, and then it is pumped up to the constant pressure liquid feeder. Here the fluid passes through a regulating valve and it is supplied at the desired flow rate to the testing cell, where it is heated up on the outer surface of the test tube. Evaporated vapor from the water films is collected into the condensers. The surplus water in the testing cell which has not been evaporated is pumped into the heating tank again.

The test tube is made of HAL77-2A aluminum brass with an outer diameter of 25.4 mm, inner diameter of 24 mm, and length of 1,600 mm. Heat flux is provided by an electric heater embedded inside the tube and the heat flux is from 0 to 3 kW.

Fig. 2 shows a simplified schematic diagram of experimental apparatus for condensation inside a horizontal tube. This apparatus is used mainly for measuring heat transfer coefficient of condensation and flow resistance of steam inside a single tube. It consists of a boiler, five test tubes in a horizontal line,

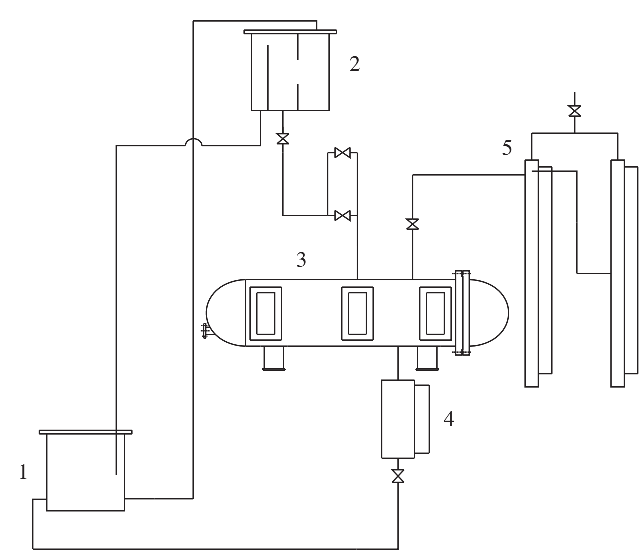

1 heating tank 2 constant pressure liquid feeder 3 evaporator
4 metering pot 5 condensers

Fig. 1. Schematic diagram of evaporation outside a horizontal tube.

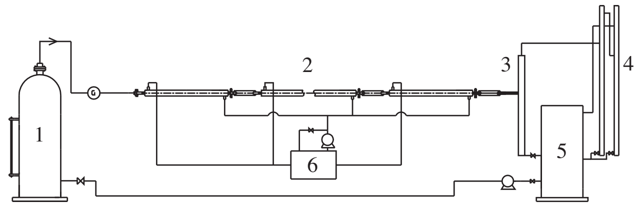

Fig. 2. Schematic diagram of condensation inside a horizontal tube.

vapor-liquid separator, two condensers, a condensate tank, and a cooling water tank. The steam in the tube exchanges heat with the cooling water and partially gets condensed. Then the mixture of steam and condensate passes through the vapor–liquid separator. Therefore the condensing rate could be measured.

Five test tubes that are made of HAL77-2A aluminum brass with an outer diameter of 25.4 mm, inner diameter of 24 mm, and length of 1,800 mm constitute the testing part of condensation heat transfer. Between every two tubes is a quartz glass tube with the length of 300 mm which is used to observe the flow pattern.

Based on the data and conclusions drawn from the two experimental setups mentioned above, some results on the overall heat transfer coefficient of horizontal-tube falling film evaporator with large tube bundle can be provided. It is supposed that the evaporator consists of 5,000 tubes, having a 25.4 mm outer diameter, 24 mm inner diameter, 8,000 mm length, which are arranged in a square-pitch layout with a pitch-to-diameter ratio of 1.3. This produces a vertical spacing of 33 mm between the tubes. The overall envelope of the tube bundle is rectangular, consisting of 50 columns of tubes with 100 tubes in each column. Calculating parameters are as follows: the evaporation temperature is 40–60℃, the spray density outside tube bundle is 0.030–0.070 $kg\,m^{-1}\,s^{-1}$, the temperature difference is 1–5℃, and the inlet steam velocity in tubes is 20–45 $m\,s^{-1}$. The present study belongs to preliminary experimental investigation, and fresh water is adopted as the experimental fluid to replace seawater for convenience, due to the unremarkable difference in h_o between fresh water and seawater in desalination [14].

3. Heat transfer performance of the evaporator

3.1. Effect of spray density and saturation temperature on overall heat transfer coefficient

Take in-tube entrance steam velocity 45 $m\,s^{-1}$ and temperature difference 3℃ for example, Fig. 3 shows the relation curve of overall heat transfer coefficient K of the evaporator and spray density Γ at different evaporation temperatures T. It can be seen that, with increasing of Γ, the K increases. On one hand, with the increment of Γ, thickness of water film increases, which can result in the rising of evaporation heat transfer resistance outside the tube. On the other hand, increment of Γ can also accelerate the liquid flow outside the tubes, which intensifies the liquid film fluctuation. It will be favorable to the convective heat transfer. Through the experiment it is found that, when Γ is between 0.030 and 0.070 $kg\,m^{-1}\,s^{-1}$, the influence of film fluctuation surpasses the influence of film thickness rise. Consequently, the increment of Γ helps to increase h_o. So when $0.030\,kg\,m^{-1}\,s^{-1} < \Gamma < 0.070\,kg\,m^{-1}\,s^{-1}$, the increment of spray density contributes to the increasing of the K.

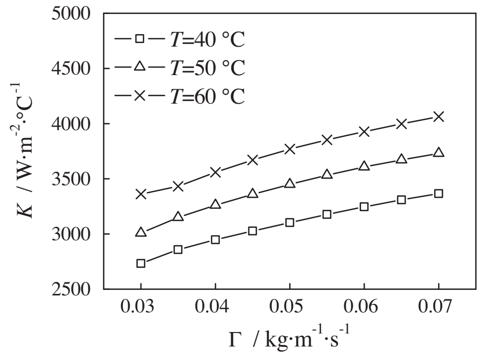

Fig. 3. Effect of spray density and saturation temperature on overall heat transfer coefficient.

From Fig. 3 we can also see that, the K increases with increasing evaporation temperature T. With the increment of T, on one hand, decreasing of the liquid viscosity leads to strengthening of liquid film turbulence outside the tubes. Besides, thickness of the liquid film also diminishes, which means that heat transfer resistance decreases. On the other hand, increment of T results in decreasing of the liquid surface tension, and the film waviness is intensified. Both the two aspects contribute to the increasing of h_o. When the total temperature difference is constant, the increment of T means increasing of condensing temperature, so viscosity and surface tension of the condensate liquid film inside the tubes decrease, which results in the growth of h_i. Thus, increasing saturation temperature is favorable to the K.

3.2. Effect of temperature difference on overall heat transfer coefficient

Fig. 4 gives the relationship between temperature difference ΔT and the K. As shown in Fig. 4, with the increasing of ΔT, the K decreases. With the increment

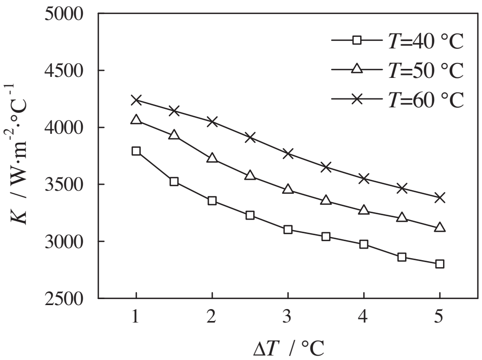

Fig. 4. Effect of total temperature difference on overall heat transfer coefficient.

of ΔT, heat flux increases and condensation liquid flow grows, which leads to the growth of thickness of liquid film inside tubes. It is unfavorable to the heat transfer process, so h_i diminishes obviously. At the same time, growth of condensate flow results in the ratio of the area of condensate at the bottom of the tube to the total heat transfer area increasing, which means that effective heat transfer area between inside and outside tubes decreases, hence h_o decreases. This result is remarkably different from some other conclusions. For completely wetted surfaces in strictly convective conditions, heat flux does not affect the heat transfer coefficient of evaporation. But under boiling-dominated conditions, the heat transfer coefficient increases with the heat flux [11]. In this paper, parameters are under strict convective evaporation condition. Therefore, the K decreases with the increasing of total temperature difference.

3.3. *Effect of steam velocity on overall heat transfer coefficient*

Fig. 5 gives the relationship between in-tube steam entrance velocity v_s and the K. From Fig. 7 it can be seen that, with the increasing of v_s, the K increases slightly. The increment of v_s is helpful to the elimination of noncondensable gas. Besides, shearing action of steam on condensate film is strengthened, which will lead to waviness of the film and diminution of film thickness. Both the two aspects help the growth of h_i. Since the heat transfer coefficient of falling film evaporation on horizontal tube is dominated by evaporation and it is not affected by the in-tube velocity, the impact of v_s on K is insignificant.

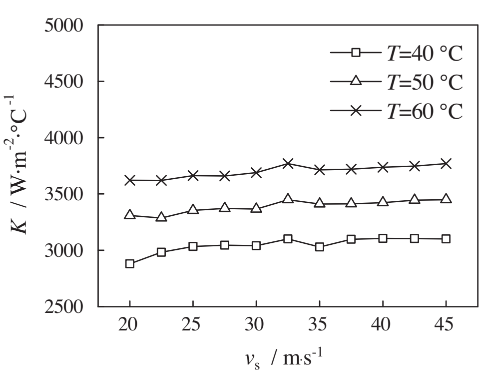

Fig. 5. Effect of steam entrance velocity on overall heat transfer coefficient.

4. Tube bundle-depth effect in the evaporator

Bundle-depth effect in the evaporator is defined as variation of local overall heat transfer coefficient $\tilde{K}$ in the vertical direction, which is plotted in Figs. 6–9, and conditions for each plot are presented in Table 1.

The influence of spray density on bundle-depth effect is demonstrated in Fig. 6. It is noted that the $\tilde{K}$ in the topmost row is the highest among all the tube rows and the $\tilde{K}$ decreases from the top row towards the bottom row. However, the effect is not very

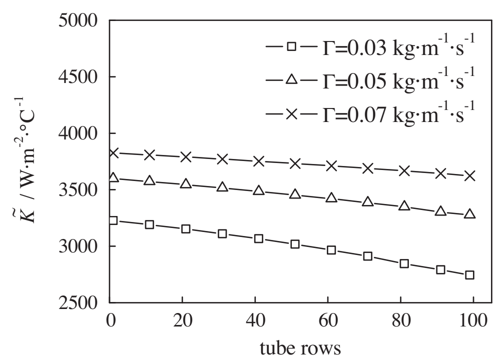

Fig. 6. Result of spray density on bundle-depth effect.

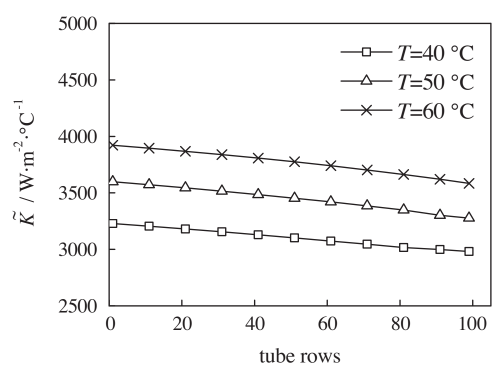

Fig. 7. Result of saturation temperature on bundle-depth effect.

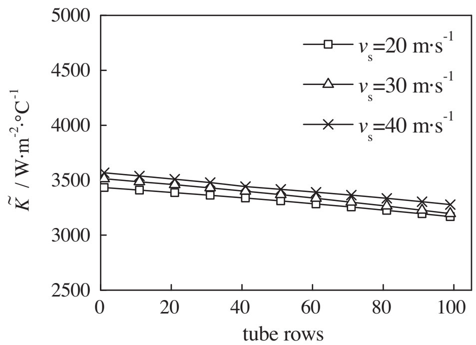

Fig. 8. Result of inlet steam velocity on bundle-depth effect.

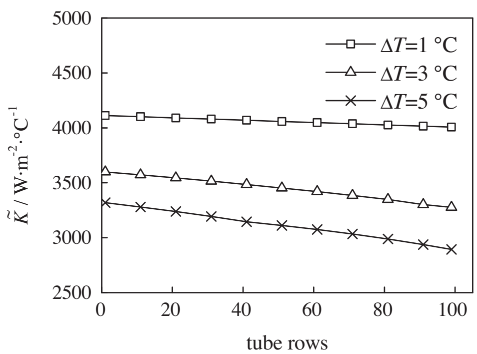

Fig. 9. Result of total temperature difference on bundle-depth effect.

Table 1
Different working conditions for Figs. 6–9

	Γ (kg m^{-1} s^{-1})	T (℃)	ΔT (℃)	v_s/m s^{-1}
Figure 6	0.03, 0.04, 0.05	50	3	45
Figure 7	0.05	40, 50, 60	3	45
Figure 8	0.05	50	1, 3, 5	45
Figure 9	0.05	50	3	20, 30, 40

noticeable at higher spray density. For instance, at $T = 50$℃, $\Delta T = 3$℃, $v_s = 45\,\text{m s}^{-1}$, the variation in the $\tilde{K}$ at $0.07\,\text{kg m}^{-1}\,\text{s}^{-1}$ is approximately 5%, while that at $0.03\,\text{kg m}^{-1}\,\text{s}^{-1}$ is about 15%. As is mentioned in Section 3.3, overall heat transfer coefficient is mainly influenced by the evaporation process, and the diminution in Γ can result in the decrease in the heat transfer coefficient. From the top row to the bottom one, film flow rate on the outer surface of the tubes is reduced due to continuous evaporation, so the $\tilde{K}$ diminishes. The lower Γ signifies the ratio of evaporated flow rate to the total flow rate rising, so variation of $\tilde{K}$ from the top to the bottom becomes large. The present result suggests that increasing Γ properly provides a high heat transfer coefficient comparatively, and the loss in the $\tilde{K}$ is also reduced.

The variation of the $\tilde{K}$ with evaporation temperature is plotted in Fig. 7. It is indicated that T almost has no impact on the bundle-depth effect. Similar results are also observed with variation inlet steam velocity, as is shown in Fig. 8. The appearance is considered to be that variations of the $\tilde{K}$ in the vertical direction is determined by the ratio between evaporation rate and the total flow rate, so the influence of saturation temperature, inlet steam velocity can be neglected. However, in Fig. 9, it is found that the bundle depth effect is weak at $\Delta T = 1$℃, which is remarkably different with that at $\Delta T = 3$℃ and $\Delta T = 5$℃. When $\Delta T = 1$℃, although the $\tilde{K}$ is high, the evaporating rate outside the tube that can affect the ratio between evaporation rate and the total flow rate is extremely small due to the relatively low temperature difference. Therefore, the variation in the $\tilde{K}$ of the vertical direction is not obvious. It is suggested that dependence of bundle-depth effect is not significant with variation of saturation temperature, and inlet steam velocity. However, spray density and total temperature difference can provide large bundle-depth effect, especially at low spray density and high temperature difference.

5. Space distribution of the $\tilde{K}$ in the evaporator

Fig. 10 gives the space distribution of the $\tilde{K}$ in the evaporator at a spray density of $0.03\,\text{kg m}^{-1}\,\text{s}^{-1}$, and evaporation temperature of 60℃, inlet steam velocity $45\,\text{m s}^{-1}$, and total temperature difference 3℃. Referring to Fig. 10, with the increment of tube rows in the vertical direction, the $\tilde{K}$ decreases. However, in the tube length direction, the $\tilde{K}$ first increases, then decreases after a maximum value.

In a horizontal-tube falling film evaporator, water is fed to the top of a bundle of heated horizontal tubes, and the fluid evaporates as it flows filmwise over the tube surfaces. The unevaporated liquid from any given tube falls onto the downward tube in the bundle, so the spray density is lower as tube rows increasing, which results in lower $\tilde{K}$ in the present experimental range.

Distribution of the $\tilde{K}$ along the tube is mainly influenced by the condensation process inside the tubes and appears rising first. When the $\tilde{K}$ reaches a maximum value, it begins to decline. On one hand, it is analyzed that enthalpy is constant from the boiler

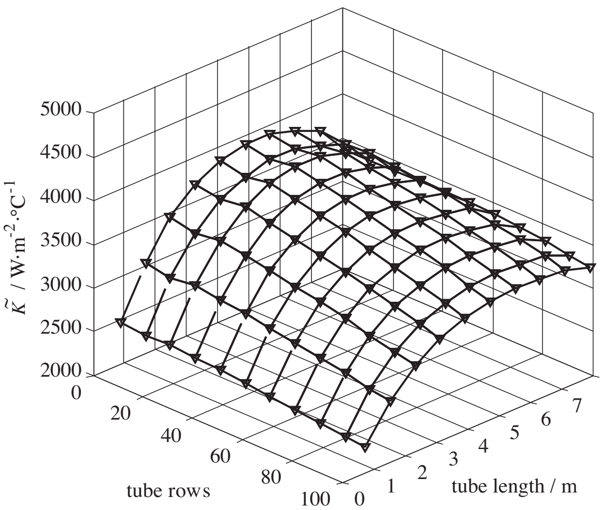

Fig. 10. Space distribution of the $\tilde{K}$ in the evaporator.

to the testing part and steam has a certain superheat because of flow resistance inside the tubes, so steam temperature is reduced to the saturation temperature after the steam enters into the tubes firstly. The above process pertains to single-phase heat exchange and the heat transfer coefficient is lower. On the other hand, through experimental observation, it is found that there is no stable condensate film formed on the tube inner surface. This appearance is more serious at higher steam velocity and it is considered that high steam velocity may decrease formation of condensation cores. Both the two aspects contribute to the lower $\tilde{K}$ at the onset part of the tube. However, influence of the two aspects becomes weak gradually and the $\tilde{K}$ increases, which reaches a peak value at about 4–5 m of the tubes and then declines. It is observed that there is obvious condensate at the bottom of the tube from 5 m to the end, which leads to decrement of effective heat transfer area. Therefore, the $\tilde{K}$ diminishes in the posterior part of the tubes.

6. Conclusions

On the basis of the experimental data outside and inside aluminum brass tubes gained from the experimental facilities, this paper presents the effect of main factors of falling film evaporation and condensation process on overall heat transfer coefficient of horizontal-tube falling film evaporator with square-pitch bundle. Bundle-depth effect and space distribution of local overall heat transfer coefficient in the evaporator are also presented. Following conclusions can be summarized briefly:

(1) Spray density and saturation temperature help to increase the K.
(2) Growth of total temperature difference leads to decreasing the K, but increment of inlet steam velocity generally acts to increase the K slightly.
(3) Dependence of bundle-depth effect is not significant with variation of saturation temperature and inlet steam velocity. However, spray density and total temperature difference can provide significant impact on the bundle-depth effect.
(4) With the increment of tube rows in the vertical direction, the $\tilde{K}$ decreases, but in the tube length direction, the $\tilde{K}$ first increases, then decreases after a maximum value.

Acknowledgment

This research is supported by the Chinese National Natural Science Foundation Projects No. 51176017 and No. 50976016.

Symbols

K — overall heat transfer coefficient of the evaporator, W m^{-2}°C^{-1}
$\tilde{K}$ — local overall heat transfer coefficient in the evaporator, W m^{-2}°C^{-1}
T — saturation temperature, °C
h — heat transfer coefficient, W m^{-2}°C^{-1}
v — velocity, m s^{-1}
Γ — spray density on one side, kg m^{-1} s^{-1}
ΔT — total temperature difference, °C

Subscripts

i — inside
o — outside
s — steam

References

[1] J.E. Miller, Review of water resources and desalination technologies, Materials Chemistry Department Sandia National Laboratories SAND 2003-0800, 2003.
[2] J.P. Chen, L.K. Wang, L. Yang, Y.-M. Zheng, Desalination of seawater by thermal distillation and electrodialysis technologies, Membr. Desalin. Technol. 13 (2008) 525–558.
[3] A. Khawaji, I. Kutubkhanah, J. Wie, Advances in seawater desalination technologies, Desalination 221 (2008) 47–69.
[4] G. Kronenberg, F. Lokiec, Low-temperature distillation processes in single- and dual-purpose plants, Desalination 136 (2001) 189–197.
[5] M.C. Chyu, A.E. Bergles, An analytical and experimental study of falling-film evaporation on a horizontal tube, J. Heat Transfer 109 (1987) 983–990.
[6] W.H. Parken, L.S. Fletcher, J.C. Han, V. Sernas, Heat transfer through falling film evaporation and boiling on horizontal tubes, J. Heat Transfer 112 (1990) 744–750.

[7] S.Q. Shen, G.T. Liang, L.Y. Gong, X.S. Mu, R. Liu, X.H. Liu, Distribution of heat transfer coefficient in horizontal-tube falling film evaporator, CIESC J. 62 (2011) 3381–3385.
[8] G.A. Jelino, Pilot Plant Test and Design Study of a 2.5MGD Horizontal-tube Multiple-effect plant, Office of Saline, Water, 1969.
[9] X. Zeng, M.C. Chyu, Z.H. Ayub, Experimental investigation on ammonia spray evaporator with triangular-pitch plain-tube bundle, part II: Evaporator performance, Int. J. Heat Mass Transfer 44 (2001) 2081–2092.
[10] X. Zeng, M.C. Chyu, Z.H. Ayub, Experimental investigation on ammonia spray evaporator with triangular-pitch plain-tube bundle, part I: Tube bundle effect, Int. J. Heat Mass Transfer 44 (2001) 2299–2310.
[11] Y. Fujita, M. Tsutsui, Experimental investigation of falling film evaporation on horizontal tubes, Heat Transfer—Jpn Res. 27 (1998) 609–618.
[12] Z.-H. Liu, Q.-Z. Zhu, Y.-M. Chen, Evaporation heat transfer of falling water film on a horizontal tube bundle, Heat Transfer—Asian Res. 31 (2002) 42–55.
[13] J.J. Lorenz, D. Yung, A note on combined boiling and evaporation of liquid films on horizontal tubes, J. Heat Transfer 101 (1979) 178–180.
[14] L. Yang, S. Shen, Experimental study of falling film evaporation heat transfer outside horizontal tubes, Desalination 220 (2008) 654–660.